Author for correspondence:
Tridib Kumar Mondal,
Emails: tridibkumarmondal@isical.ac.in;
tridibkumarmondal@gmail.com

CAMBRIDGE
UNIVERSITY PRESS

Magnetic shape fabric analysis from syntectonic granites: a study based on the eigenvalue method

Sankha Subhra Acharyya[1] and Tridib Kumar Mondal[2]

[1]Centre for Earth Sciences (CEaS), Indian Institute of Science, Bengaluru 560012, India and [2]Geological Studies Unit, Indian Statistical Institute, West Bengal 700108, India

Abstract

We investigate the shape and strength of the magnetic fabrics (anisotropy of magnetic susceptibility (AMS) data) of various massive granitic plutons from different parts of India, using the eigenvalue method. The study aims to analyse eigenvalues and establish their relationship with various deformational attributes. It involves: (1) calculating eigenvectors and their corresponding eigenvalues from magnetic fabric datasets; (2) finding a link between the geometrical appearance of eigenvectors and the mechanistic issues involved with a specific deformation scenario; and (3) determining shape and strength parameters from the magnetic foliation data distribution.

The statistical analysis for the unimodal magnetic fabric dataset of orthorhombic symmetry class implies that the plane, consisting of intermediate (V_2) and minimum (V_3) eigenvectors with pole V_1, accurately traces the instantaneous stretching axis (ISA_{max}) of a particular material flow system under a pure shear regime. Moreover, for the distributions of similar symmetry and modality, we infer that the rotational characteristics of eigenvectors with respect to a fixed coordinate cause a distinct shift of such planes (V_2–V_3) from the ISA_{max} of a steady-state flow system under simple shear, where a substantial amount of rotational strain is involved. However, our findings also suggest that variation in symmetry and modality of magnetic fabric data distribution of different studied granitoids can directly influence the relative disposition of V_2–V_3 with respect to the direction of ISA_{max}. We conclude that eigenvalue analysis of magnetic fabrics is a powerful approach, which can be utilized while studying the salient deformational aspects of any syntectonic massive granitic body.

1. Introduction

Shape fabric analysis is an important aspect to unravel the complex geological structures and determine the state of strain in rocks (Woodcock, 1977; Cobbold & Gapais, 1979). Various methods have been used to investigate shape fabrics, such as stereographic projection, eigenvalue calculations, and anisotropy of magnetic susceptibility (AMS) measurements (e.g. Woodcock, 1977; Cobbold & Gapais, 1979; Launeau *et al.* 1990; Simpson & De Paor, 1993; Tikoff & Fossen, 1995; Wallis, 1995; Launeau & Robin, 1996; Olivier *et al.* 1997; Grasemann *et al.* 1999; Gomez-Rivas *et al.* 2007). Amongst these methods, the eigenvalue method is a powerful tool which provides detailed information about the shape as well as the strength of the fabrics. It also helps to quantify the degree of randomness, both arithmetically and graphically (Williams & Chapman, 1979; Woodcock & Naylor, 1983).

AMS is often measured to quantify the fabric of low-anisotropy rocks, i.e. rocks which do not show any mesoscopic field foliation such as granite, quartzite etc. (Owens & Bamford, 1976; Tarling & Hrouda, 1993; Borradaile & Henry, 1997; Bouchez 1997; Borradaile & Jackson, 2004; Mondal & Mamtani, 2013). AMS helps to understand the deformation and strain variation in a rock and establish the tectonic history of a region (Mamtani & Greiling, 2005; Almqvist *et al.* 2014; Ferré *et al.* 2014; Mondal & Mamtani, 2014 and references therein). AMS involves inducing a magnetic field in a sample in different directions and measurement of the induced magnetization in each direction (Tarling & Hrouda, 1993). The orientation and magnitude of the three principal axes of the AMS ellipsoid allow the magnetic planar and/or linear fabric to be determined.

Although AMS provides information about the magnetic fabrics, it is challenging to relate it to deformation in case of poly-deformed rocks. In superposed deformation, the early formed magnetic foliation in rocks may be reoriented and become very weak. Thus, it is crucial to quantify these fabrics in light of regional deformation. The eigenvalue method helps to analyse such fabrics using few parameters. Collectively, most of the previous studies performed on the geological application of AMS methods show a lack of clear assessment of the correlation between eigenvector analysis of AMS data and its connection with the mechanistic issues related to

regional tectonics. Of a few studies that have addressed such topic, Parés *et al.* (1999) used eigenvector analysis of AMS data to link magnetic fabric development with the progressive deformation in mud rocks. In this regard, Pueyo *et al.* (2004) also discussed the utilization of normalized eigenvalues in order to analyse magnetic fabric statistics of paramagnetic granites.

In the present paper, we use published AMS data from five different granitoids of India and analyse them using the eigenvalue method to quantify their degree of relative randomness. The present investigation uses the following steps: (1) calculation of eigenvalues and corresponding eigenvectors from the 'orientation tensor matrix'; and (2) determination of shape and strength parameters from the magnetic foliation data. The study graphically quantifies the degree of randomness of poles to magnetic foliation.

2. Shape fabric analysis using eigenvalue method – the background

In geology, the characterization of directional data along with their relative attitude, randomness and shape are crucial. For a large-array dataset, overlap between data is common and their representation becomes challenging. Therefore, an approach consisting in specifying directional features by a limited number of representative parameters should avoid this large-array problem. Shape fabric analysis is very useful method in representing such a dataset. Attributing these representative parameters can be solved using a procedure that involves a tensor matrix determined from the dataset, and from which eigenvectors and eigenvalues may be calculated (Watson, 1966; Mark, 1973, 1974; Owens, 1973; Mark & Andrews, 1975; Woodcock & Naylor, 1983).

Before diving into main purpose of the current study, we would like to briefly refer to some well-known previously proposed methods of shape fabric analysis. In order to depict the preferred orientation of tectonically strained objects, Flinn (1965) established a diagram, having the 'maximum/intermediate' and 'intermediate/minimum' as its vertical and horizontal axes, respectively, which has been of immense interest to structural geologists till today. Subsequently, Woodcock (1977) introduced another spherical data analysis method, termed as the 'Flinn–Woodcock plot', by integrating the shape of ellipsoid with the distribution type (i.e. cluster/great-circle girdle) of the orientational data. In addition to these, other interesting methods of analysing the fabric shapes were proposed by Jelínek (1981), which not only described the type of magnetic anisotropy, but also addressed some important issues associated with the anisotropic concentration of orientational data. Borradaile (2003) provided an in-depth review of several methods of spherical-orientation data analysis, relating to sampled AMS data distribution in time, space and orientation.

However, it may be noted that these studies were all restricted to the fabric shapes originating from the single deformation event and provided scope to further study the more complex, multi-modal data distributions, which are the product of some specific regional tectonics.

In this present study, we perform the eigenvalue analysis method and analyse magnetic fabrics of different syntectonic granitic plutons from different parts of India to comment on the variation of magnetic shape fabric from a coaxially deformed region to a non-coaxially deformed one. As Scheidegger (1965) and Woodcock (1977) provide a detailed description of the theoretical basis of this eigenvalue method, we present here only the salient aspects of the principle involved in shape fabric analysis. The eigenvalue method assumes that each orientation is represented by a unit vector. Therefore, a 3×3 matrix, called an 'orientation tensor matrix', is formed by taking the summation of the cross-products of the direction cosines of unit vectors (Scheidegger, 1965).

$$a = \begin{vmatrix} \sum l^2 & \sum lm & \sum ln \\ \sum ml & \sum m^2 & \sum mn \\ \sum nl & \sum nm & \sum n^2 \end{vmatrix}$$

A normalized form of this matrix (A) is given below:

$$A = a/N.$$

where, N is the number of data; l, m and n are the direction cosines of a particular unit vector. Further, the eigenvectors (v_1, v_2 and v_3) and their corresponding eigenvalues (λ_1, λ_2 and λ_3) are determined from the above tensor matrix. The maximum eigenvector v_1 represents the direction along the minimum 'moment of inertia' of the distribution, while v_3 indicates maximum 'moment of inertia' (Watson, 1966). The eigenvalues are used mainly in their normalized form:

$$S_1 + S_2 + S_3 = 1, \text{ where } S_i = \lambda_i/N.$$

These normalized eigenvalues are directly related to the shape of the fabric, as the clusters and girdles in equal-area projection of a distribution consist of $S_1 > S_2 \sim S_3$ and $S_1 \sim S_2 > S_3$, respectively (Watson, 1966).

The last step of this analysis involves the calculation of two parameters from the graphical presentations of S_1, S_2 and S_3: (i) The shape parameter (K), which can be obtained by plotting the $\ln(S_2/S_3)$ vs $\ln(S_1/S_2)$, similar to the Flinn diagram (Flinn, 1962); and (ii) the strength parameter (C) defined by $\ln(S_1/S_3)$ which quantifies the randomness of the distribution.

In the present paper, we use the above two parameters, and position of the eigenvectors on the equal-area projection of the poles to the magnetic foliations corresponding to the primary dataset coming from different granitoids of India. The randomness is quantified, and this is followed by an assessment of the shape of the distribution data in the light of their regional tectonics. Figure 1 shows the step-wise procedure of the above-described calculations applied to the poles to magnetic foliations (K_3) represented by their plunge (P) and trend (T) coming from the Chakradharpur granite (India).

3. Available data

As already mentioned, we have used the AMS data from five granite bodies, namely Chakradharpur, Godhra, Malanjkhand, J. N. Kote and Chitradurga, located in various parts of India (see Fig. 2). Extensive AMS studies have been carried out in the above regions. All the granites have been inferred to be syntectonic with regional deformation and associated with regional-scale shear zones in their respective vicinities. Below we provide available data which are only salient for the present analysis.

3.a. Chakradharpur granitoid

The magnetic fabric in this Precambrian granitoid has developed syntectonically along with the evolution of the Singhbhum Shear
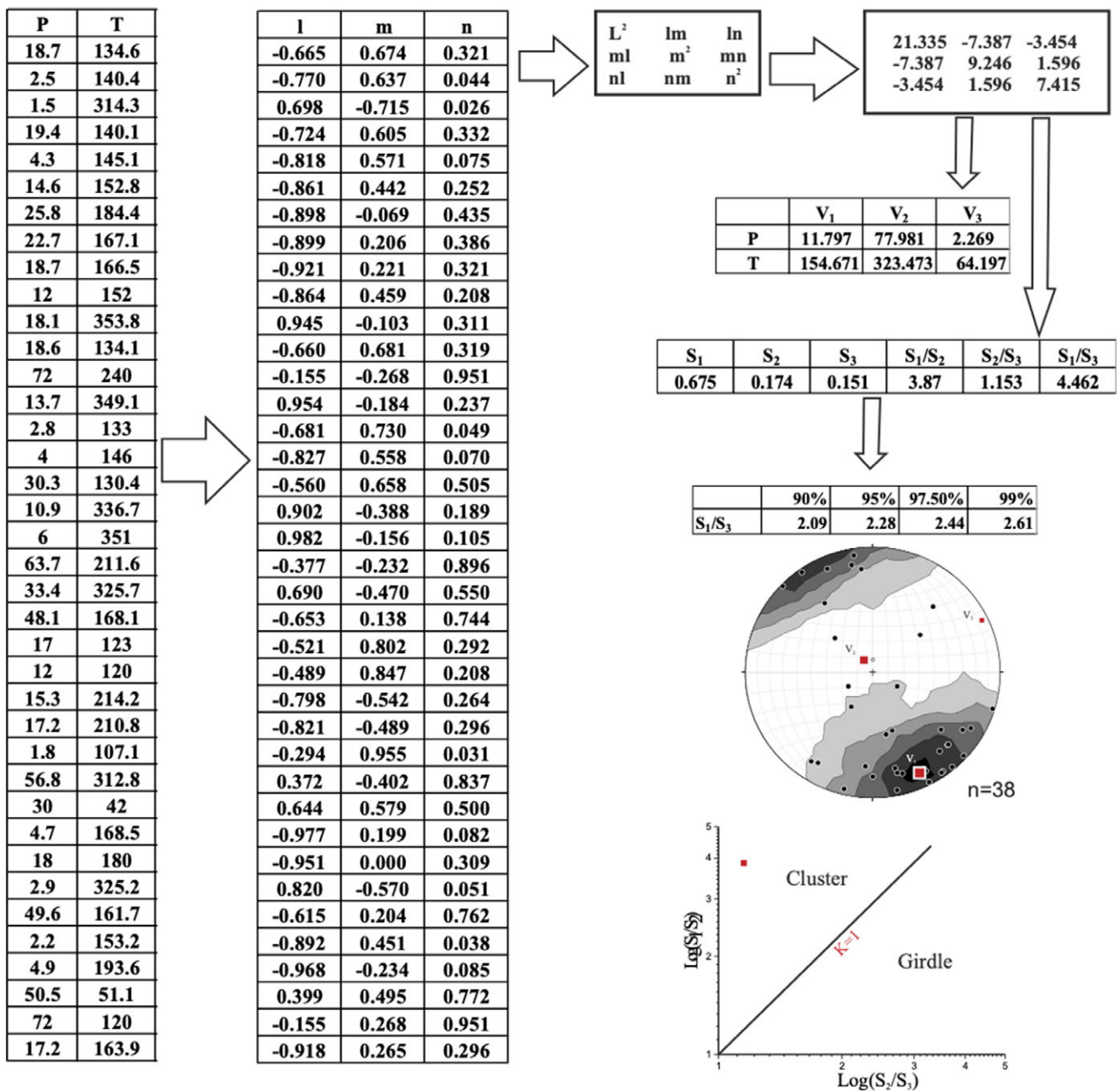
P	T
18.7	134.6
2.5	140.4
1.5	314.3
19.4	140.1
4.3	145.1
14.6	152.8
25.8	184.4
22.7	167.1
18.7	166.5
12	152
18.1	353.8
18.6	134.1
72	240
13.7	349.1
2.8	133
4	146
30.3	130.4
10.9	336.7
6	351
63.7	211.6
33.4	325.7
48.1	168.1
17	123
12	120
15.3	214.2
17.2	210.8
1.8	107.1
56.8	312.8
30	42
4.7	168.5
18	180
2.9	325.2
49.6	161.7
2.2	153.2
4.9	193.6
50.5	51.1
72	120
17.2	163.9

l	m	n
-0.665	0.674	0.321
-0.770	0.637	0.044
0.698	-0.715	0.026
-0.724	0.605	0.332
-0.818	0.571	0.075
-0.861	0.442	0.252
-0.898	-0.069	0.435
-0.899	0.206	0.386
-0.921	0.221	0.321
-0.864	0.459	0.208
0.945	-0.103	0.311
-0.660	0.681	0.319
-0.155	-0.268	0.951
0.954	-0.184	0.237
-0.681	0.730	0.049
-0.827	0.558	0.070
-0.560	0.658	0.505
0.902	-0.388	0.189
0.982	-0.156	0.105
-0.377	-0.232	0.896
0.690	-0.470	0.550
-0.653	0.138	0.744
-0.521	0.802	0.292
-0.489	0.847	0.208
-0.798	-0.542	0.264
-0.821	-0.489	0.296
-0.294	0.955	0.031
0.372	-0.402	0.837
0.644	0.579	0.500
-0.977	0.199	0.082
-0.951	0.000	0.309
0.820	-0.570	0.051
-0.615	0.204	0.762
-0.892	0.451	0.038
-0.968	-0.234	0.085
0.399	0.495	0.772
-0.155	0.268	0.951
-0.918	0.265	0.296

L^2	lm	ln
ml	m^2	mn
nl	nm	n^2

21.335	-7.387	-3.454
-7.387	9.246	1.596
-3.454	1.596	7.415

	V_1	V_2	V_3
P	11.797	77.981	2.269
T	154.671	323.473	64.197

S_1	S_2	S_3	S_1/S_2	S_2/S_3	S_1/S_3
0.675	0.174	0.151	3.87	1.153	4.462

	90%	95%	97.50%	99%
S_1/S_3	2.09	2.28	2.44	2.61

n=38

Cluster

K=1

Girdle

$Log(S_1/S_2)$

$Log(S_2/S_3)$

Fig. 1. (Colour online) Stepwise procedure for eigenvector analysis (Woodcock & Naylor, 1983) from pole to magnetic foliation (K_3) data (Mamtani et al. 2013).

Zone (SSZ) that lies to its south (Mamtani et al. 2013). The Chakradharpur granitoid lacks well-developed magmatic fabrics, and the mean magnetic susceptibility (K_m) varies from 67.6 to 659 µSI (Table 1). It has been inferred that biotite is the main para-magnetic phase contributing to its AMS (Mamtani et al. 2013). The mean magnetic foliation plane (K_1K_2) has an orientation of N54°E (strike) with a steep to vertical dip (Fig. 2a). Mamtani (2014) has performed a 2D vorticity analysis and concluded that the fabric of this granite body is dominated by pure shear (kinematic vorticity number $W_k = 0.58$) and associated with the evolution of nearby shear zone.

3.b. Malanjkhand granitoid

AMS measurements have been performed in the ~2.48 Ga Malanjkhand body (Fig. 2b) in order to evaluate the time relationship between fabric development in the granite and the regional tectonics (Majumder & Mamtani, 2009). The Central Indian Suture (CIS) that defines the southern margin of the Central Indian Tectonic Zone (CITZ) demarcates the NW boundary of this granite body. The magnetic fabric trajectory that can be drawn in the Malanjkhand granite is interpreted to be related to synmagmatic deformation (Majumder & Mamtani, 2009). Mamtani (2014), has previously identified two prominent sectors
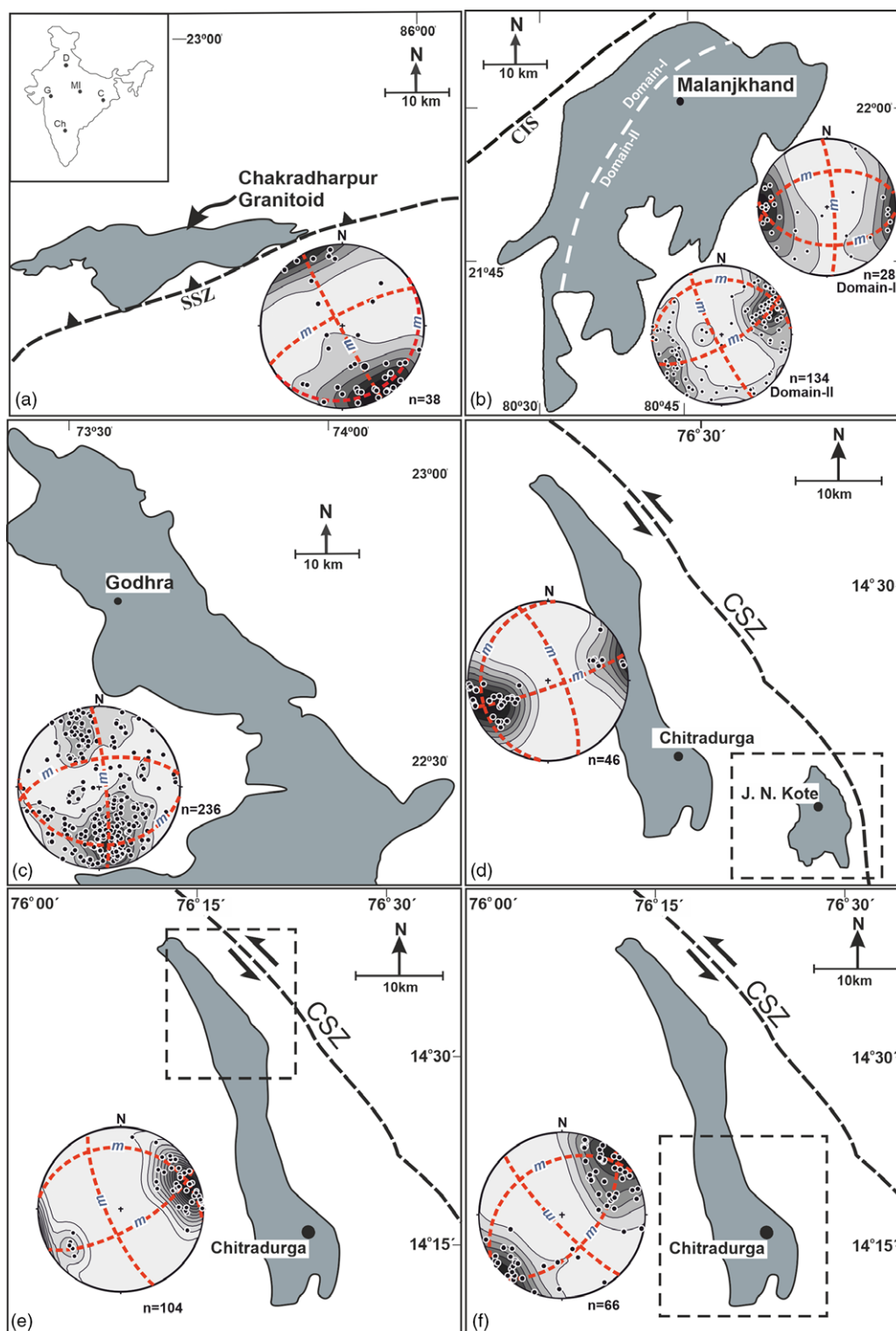
Fig. 2. (Colour online) Location map of the various younger granites from Indian continent. (a–d) Regional maps of Chakradharpur (Mamtani *et al.* 2013) (a), Malanjkhand (Majumder & Mamtani, 2009) (b), Godhra (after Sen & Mamtani, 2006) (c) and J. N. Kote (Mondal & Mamtani, 2014) (d) granitoids. (e, f) Map of Chitradurga granites (Mondal, 2018). Dashed boxes in (e) and (f) are the northern and southern part of the granite, respectively. Inset in (a) shows the locations of these granitoids in the map of India. The lower-hemisphere equal-area projection in each panel shows the pole (K_3) to magnetic foliation and their corresponding symmetry arguments. Planes of symmetry (m) are shown as dashed red lines in each of the stereonets. Software StereoNet (Allmendinger *et al.* 2013; Cardozo and Allmendinger, 2013) was used for all lower-hemisphere equal-area projection and contouring (http://www.geo.cornell.edu/geology/faculty/RWA/programs/stereonet.html). Dashed black lines in (a), (b), (d), (e) and (f) show the trend of regional shear zone.

(domain-I and domain-II) in Malanjkhand granite based on their spatial disposition with respect to the adjacent CITZ. The K_m shows a variation from 190.8 to 3490.5 µSI in domain-I. However, for domain-II, this range is found from 268.47 to 5789.62 µSI (Table 1). It is also interpreted that domain-I and domain-II are pure- ($W_k = 0.98$) and simple-shear ($W_k = 0.34$) dominated, respectively.

3.c. Godhra granitoid

The Godhra body (955 ± 20 Ma) is known to have developed its fabric synchronously with Grenvillian-age tectonic rejuvenation of the Central Indian Tectonic Zone (CITZ) that lies to its south (Fig. 2c). AMS studies have revealed that the paramagnetic minerals, namely biotite and in some samples hornblende, and the ferromagnetic (*sensu lato*) magnetite are the important phases that

Table 1. Characterization of every granitic body

Granitic body	Emplacement age	Deformation age(s)	AMS sites (N)	Info of Bulk K			Mean K_1		Mean K_3		NRM info
				% of sites	K_{mean} ($\times 10^{-6}$ SI)	σ_K ($\times 10^{-6}$ SI)	dec. (°)	inc. (°)	dec. (°)	inc. (°)	
Chakradharpur granite	Archaean: ~3100 Ma	Synmagmatic, with the evolution of SSZ	38	~88	67.6	39.01	40	63	144	1	NA
				<12	659	124.5					
Malanjkhand granite (domain-I)	Palaeo-Protero –zoic: ~2480 Ma	Syn-magmatic. Fabric development, influenced by Palaeo-Proterozoic CITZ	28	>92	190.08	65.89	238	85	275	10	NA
				<8	3490.5	2729.5					
Malanjkhand granite (domain-II)			134	~44	268.47	88.42	283	83	65	22	NA
				~58	5789.62	5075.84					
J.N.Kote Granite	2560–2507 Ma	Same as Point no. 6, 7 (see below)	46	100	69.85	25.99	354	44	253	12	NA
				–	–	–					
Godhra granite	955 ± 20 Ma	Synchronous with Grenvillian-age tectonic rejuvenation of CITZ	236	>58	169.07	91.4	322	24	165	19	NA
				<42	5756	4142.8					
Chitradurga granite (South)	2614 ± 10 Ma	Late Archaean ductile, transpressive, coaxial D1 and D2, followed by late-stage brittle D3 event	66	~58	138.42	79.67	250	78	47	04	NA
				<42	1289.06	696.09					
Chitradurga granite (North)			52	>88	116.69	73.85	192	75	76	25	NA
				<12	585.14	46.8					

K_m = mean susceptibility; σ_K = standard deviation of magnetic susceptibility; K_1 = magnetic lineation; K_3 = pole to magnetic foliation – shaded regions for each studied granite depict % of sample sites, having ferromagnetic character. References for available data: Chakradharpur (Mamtani *et al.* 2013); Malanjkhand (Majumder & Mamtani, 2009); Godhra (Sen & Mamtani, 2006); J. N. Kote (Mondal & Mamtani, 2014); Chitradurga (South) and Chitradurga (North) (Mondal, 2018).

contribute to the AMS (Mamtani & Greiling, 2005). The magnetic foliation in the Godhra granite body is dominantly ENE–WSW in orientation (Fig. 2b), i.e. parallel to the CITZ (Sen & Mamtani, 2006). K_m values vary widely from 169.07 to 5756 μSI. Recently, Mamtani (2014) concluded that the late-stage fabric in this magmatic body was dominated by pure shear ($W_k = 0$).

3.d. J. N. Kote granitoid

This Archaean-age granite body (Fig. 2d) is located in the vicinity of the Chitradurga granite (Fig. 2e) and was emplaced syntectonically during the evolution of the adjacent Chitradurga Shear Zone (CSZ). AMS was performed on this granite (Mondal, 2018) and the magnetic fabric is found to be parallel to the CSZ. Their susceptibility (K_m), being ~69.85 μSI, indicates a dominant contribution of paramagnetic phases. The magnetic fabric of the J. N. Kote body is interpreted to be dominantly due to simple shearing ($W_k = 0.80$) that occurred during its emplacement along the granite–TTG contact (Mondal, 2018).

3.e. Chitradurga granitoid

The fabric in granite (~2.6 Ga) from the Chitradurga region (Western Dharwar Craton, south India; Fig. 2e, f) is analysed using AMS study (Mondal, 2018; Mondal *et al.* 2020). The microstructural investigation on the granite shows a progressive textural overprint from magmatic, through high-T to low-T solid-state deformation textures. The mean magnetic foliation in the rocks of the region is dominantly NW–SE-striking. K_m values range from 138.42 to 1289.06 μSI in the southern region, while in the northern region they vary from 116.69 to 585.14 μSI. The vorticity analysis from magnetic fabric in the southern region of the Chitradurga granite reveals that the NW–SE-oriented fabric formed under pure shear condition ($W_k = 0.06$; Mondal, 2018; dashed box in Fig. 2e). However, the northern region of the granite is closed to the adjacent CSZ and is inferred to be controlled by simple shearing ($W_k = 88$; dashed box in Fig. 2f).

Based on the available magnetic dataset, each granitic body is characterized in Table 1 (see table caption for references) by its emplacement as well as deformation age(s), number of AMS stations, mean bulk susceptibility (K_m and the information on standard deviation), and declination and inclination of mean K_1 and K_3. This characterization, inturn, embodies the basis for two initial important assumptions made for this study which are discussed in Section 4.

We also use the magnetic foliation data to quantify the degree of randomness of the fabric under this study. The study also helps us to understand the mode of shearing (simple/pure) responsible for the development of the magnetic fabrics in the corresponding areas. Details of this application of magnetic fabric using the eigenvalue method are presented in Section 5.

4. Initial assumptions made in the current analysis

Prior to discussing the application of the present study, we epitomize the twofold aspects of our assumptions in the following subsections.

4.a. Behaviour of granitic bodies under respective regional deformation

The granitoids analysed in this study are replete with structural fabric which has developed during their syntectonic emplacement

on account of corresponding regional tectonics. These granitic plutons show superimposition of low-temperature deformation textures over high-temperature and that developed uniformly when the granites cooled from high temperature to low temperature.

In the case of Malanjkhand (Majumder & Mamtani, 2009) and Godhra granite (Mamtani & Greiling, 2005), the magnetic foliations (K_3) not only fit well with the field fabric orientation of the two granites, but also show similarities to that of the older gneiss adjacent to their margin. The magnetic lineation (K_1) is found to be consistent and uniform even in a large domain (kilometre-scale). Furthermore, the presence (having overall consistency in stretching lineation at km scale) and absence of mylonite, respectively, in domain-I and domain-II of the Malanjkhand granite (shown in Fig. 2b) support the uniform and unique behaviour of each, while responding to the syntectonic cooling that succeeded their emplacement. A discussion on the kinematics of Chakradharpur granite (Mamtani *et al.* 2013) reveals that the granite preserves an oblique relationship between its magnetic and field foliation, interpreting the development of the former in the crystallization stage. Besides, the field foliation of the granite has been found parallel to the adjacent shear zone (SSZ) orientation located in its southern margin, indicating that the magnetic and field fabrics of this granite 'froze' as succeeding events under the progressive deformation linked to its syntectonic crystallization. According to Mondal (2018), the other three studied granites i.e. Chitradurga (South), Chitradurga (North) and J. N. Kote, also preserve micro- and mesoscale features that are similar to the Malanjkhand and Godhra granite. This study confirms the existence of parallelism between magnetic foliations in these and a regional trend of the adjacent shear zone (CSZ) as well as field foliations measured from adjacent metasedimentary rocks. Moreover, shape preferred orientation (SPO) analysis, performed by the same author on recrystallized sub-grains of stretched quartz, demonstrates that their long-axis orientation exactly traces the magnetic foliations, which are again found to be in good agreement with the regional stress states associated with these three granites (Mondal, 2018).

Bearing in mind the above-discussed information related to all of our studied granites (or part, as in Malanjkhand pluton), we assume that they behaved in a uniform and homogeneous way in order to record an overall shear type (pure/simple) during their corresponding regional deformation. Indeed, the pluton-scale estimation of different kinematic vorticity numbers (see their values in Section 3) from the granitoids or any domain of it is also found to be in line with our assumption.

In this connection, considering the main characteristics of K_3 data on the stereonet, such as well-defined girdles or strong maxima (the latter in our case) at the pluton scale, we observe that there exist three mutually orthogonal planes of symmetry for all the analysed granites (Fig. 2 insets). As suggested by Paterson and Weiss (1961), this feature of the stereonet pattern can be used to interpret the overall orthorhombic symmetry (Bingham, 1974) of structural fabric at larger scale (pluton scale, here), even if any deviation (monoclinic/triclinic/axial, etc.) may exist at the metric or decametric site scale as a result of natural variability, including local response to deformation. Likewise, extrapolation of any small-scale symmetry pattern seems not to be always rational when assessing the structural dataset over a comparatively large scale.

Since no field observations have marked occurrences of significant local stress-induced perturbations in any of the studied

plutons, we trust in the mutual orthogonality of three symmetry planes to infer the overall orthorhombicity of the magnetic foliation dataset at the pluton scale for each granite.

4.b. AMS ellipsoid and its relation to the rock fabric

The relationship between AMS ellipsoid and rock fabric (or mineral preferred orientations) has long been an absorbing subject of discussion, and provides the final basis of our assumptions in the present study. Several research (Rochette, 1987; Bouchez, 1997), that thematically targeted granitic bodies with regard to this particular issue, clearly revealed that this relationship can be granted for case where paramagnetic minerals make a dominant contribution to the bulk magnetic susceptibility (K) of a granitic body. Although the interpretation of ferromagnetic and paramagnetic data may differ substantially (Trindade *et al.* 1999; Terrinha *et al.* 2017). Especially when the contribution of iron-phyllosilicates (such as biotite, amphibole, etc.) defines the K of a granite, their magneto-crystalline anisotropy gives rise to parallelism between their magnetic axes and crystallographic axes (and therefore their shape axis) (Martín-Hernández and Hirt, 2003). However, in comparison with such granites where AMS can directly be utilized as a strain indicator, drawing similar correlations is somewhat complicated for ferromagnetic-dominated (magnetite-bearing) granites. This is due to the functioning of other factors such as a strong control of magnetite content on K (Benn *et al.* 1993) and the 'interaction anisotropy' (Grégoire *et al.* 1995). In the present study, information on bulk mean-magnetic susceptibility (K_m and its standard deviation) for different granitoids is subcategorized in Table 1 according to the percentage of their AMS sites whose samples show either a paramagnetic or ferromagnetic character. Bouchez (1997) stated that granites with $K_m < 500$ μSI can be interpreted as paramagnetic granites whereas the others ($K_m > 500$ μSI) are referred to as ferromagnetic. Based on this, Chakradharpur, Malanjkhand (domain-I), J. N. Kote and Chitradurga (North) granites (column 1 of Table 1) show that samples from ~90% of these sites are paramagnetic, whereas very few (~8–12 %) appear to be ferromagnetic, so they behave as overall paramagnetic-dominated granites. However, for the rest of the granites (such as Malanjkhand (domain-II), Godhra and Chitradurga granite (South)), ferromagnetic samples are observed in a substantial percentage (~58 %) of sites, with paramagnetic ones in <42–44 % of sites. It has also been previously established for all granites that the iron-phyllosilicate such as biotite (and hornblende in a few samples) was the main paramagnetic phase in contributing to the development of magnetic susceptibility, whilst magnetite (*sensu lato*) acted as an important ferromagnetic contributor to the AMS (see individual references for each granite in Table 1 caption). Taking account of the probable influence of magnetite content on the magnetic fabric, we observe that magnetic anisotropy (K_m vs P'; after Jelínek, 1981) scatterings for ferromagnetic samples do not provide any one-to-one relationships for Malanjkhand (domain-II), Godhra and Chitradurga (South) granite (Supplementary figure 1, available online at https://doi.org/10.1017/S0016756822000747). Furthermore, lower-hemisphere equal-area projections of K_3 orientations for all ferromagnetic samples confirm their resemblance with respect to that in paramagnetic samples (Supplementary figure 2, available online at https://doi.org/10.1017/S0016756822000747). This information therefore allows us to conclude that so far as the orientations of magnetic foliation are considered, the magnetite content of these

granites does not remarkably create noise in the contribution of paramagnetic phases to the AMS.

In addition, ore petrography of the paramagnetic samples clearly revealed that the opaque phases present in all the studied granites are goethite, pyrite and hematite, excluding magnetite. These studies also concluded that magnetite (for all the granites) displays 'Verwey Transition' (Tarling & Hrouda, 1993) in the cooling experiments, indicating their Multidomain (MD) characteristics. This finally helps us to eliminate the possibility of inverse fabric development in the studied granitoids. Based on the above discussions, we have preferably assumed that the magnetic fabric dataset used in the current study records mineral (or shape) preferred orientation and hence provides the strain information directly for each of the studied plutons.

5. Results

The published magnetic data (poles to magnetic foliation) from Chakradharpur, Malanjkhand (domain-I and -II), Godhra, J. N. Kote, northern and southern Chitradurga granite are analysed using the eigenvalue method. In Fig. 2 (insets), the positional individuality of characteristic eigenvectors, calculated (arithmetically) from orientation tensor matrices (see Fig. 1, third and fourth steps) using the available dataset, is depicted on the contoured lower-hemisphere equal-area projection of poles to magnetic foliation for each granitoid, separately.

It may be noted that all the granitoids show orthorhombic fabric symmetry classes, where the position of the maximum eigenvector (V_1), for each granitoid exhibits their tendency to overall trace the densest area of data distribution on stereonets (Fig. 2, inset).

In Fig. 3, the attitude of the plane containing the intermediate and minimum eigenvector (i.e. the V_2–V_3 plane) is separately portrayed to determine its relative disposition with respect to mean magnetic foliation (MF) and shear zone, for individual granitoid. It is clearly evident from Fig. 3b1 and e that the strike of the V_2–V_3 planes for the pure-shear-dominated regions, such as Malanjkhand domain-II and southern Chitradurga, exactly mimics the strike of MF planes. Conversely, in the simple-shear-dominated regions such as Malanjkhand domain-I, J. N. Kote and northern Chiradurga, the relationship between V_2–V_3 and MF does not hold with the aforementioned observation, as a distinct shift of the strike of the V_2–V_3 planes from that of the MFs may be noted in Figure. 3b2, c and f, respectively. The angular difference between the strikes of V_2–V_3 and MF in these three granitoids is found to be 10°, 5° and 9°, respectively. Interestingly, however, the other two studied granitoids i.e. Chakradharpur and Godhra (the shaded region in the Fig. 3), exhibit an eccentric relationship between their V_2–V_3 and MF directions, contrary to our observations both in Figure 3b1 and e and in Figure 3b2, c and f. Despite being a pure-shear-dominated region, the V_2–V_3 plane of Godhra granite shows a marked angular variation (6°) from its MF plane's strike. Also, Chakradharpur, which is a general-shear-dominated region, reflects greater angular variation (~11°) between the strikes of its V_2–V_3 and MF than what we previously observed in other simple-shear-dominated regions. Figure 3 (inset), where the angular relationships (between V_2–V_3 and MF) of all granitoids are plotted against their vorticity numbers, also clearly reflects such eccentricities observed in the two granitoids (see the shaded elliptical region in Fig. 3 in-set). For the other granitoids, the angular shift of the V_2–V_3 plane from MF's orientation linearly increases with a
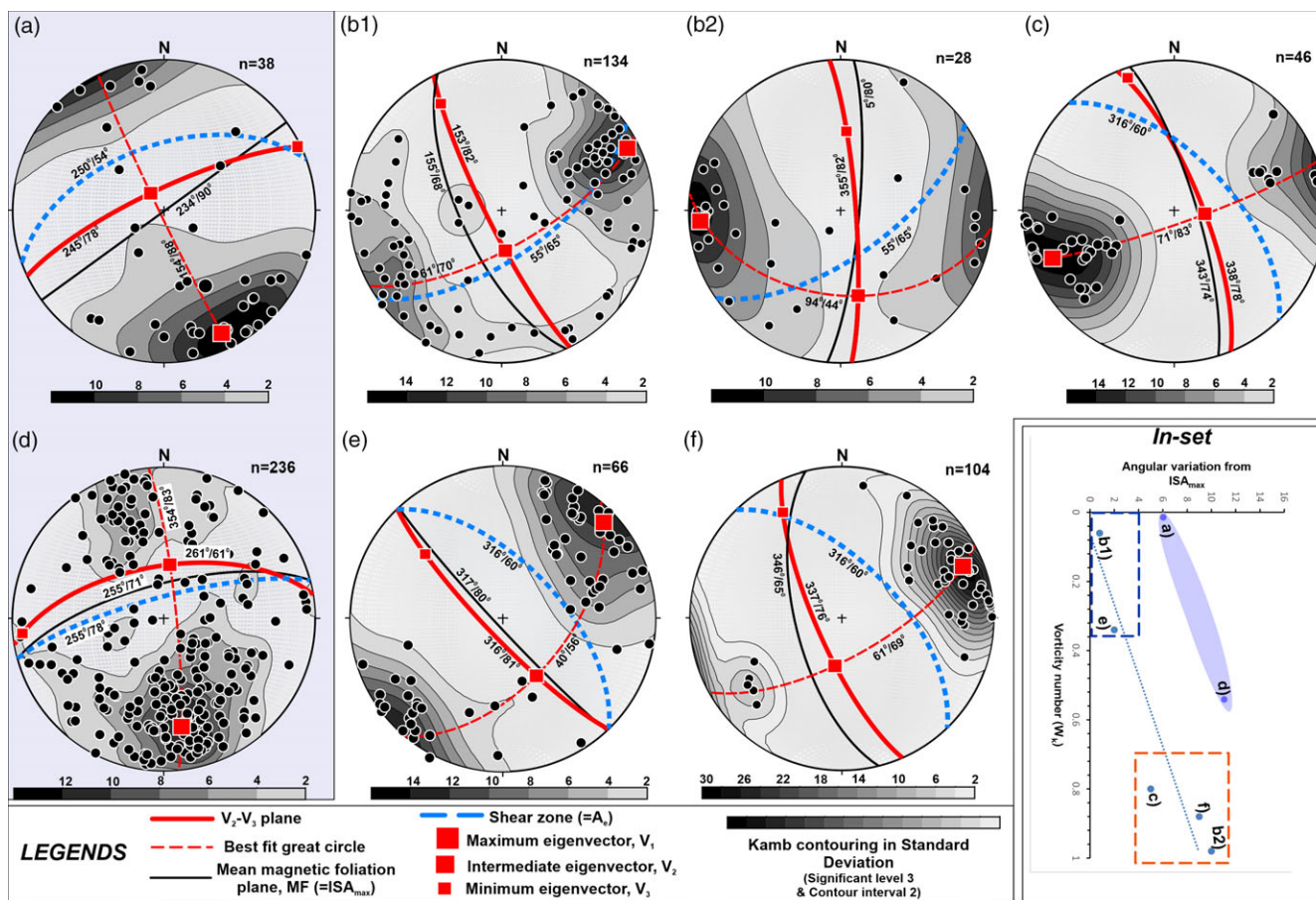
Fig. 3. (Colour online) Superimposition of V_2–V_3 planes and best-fit great circles (see legends) on lower-hemisphere equal-area projections of pole to magnetic foliation (K_3) for each individual granitoid, depicting their relations with the corresponding mean magnetic foliation planes (MF) and the flow apophyses directions of extension (A_e = shear zone). The positional uniqueness of eigenvectors amid the K_3 data distributions is also exhibited in each panel. (a), (b1), (b2) (c), (d), (e) and (f) denote Chakradharpur, Malanjkhand (domain-II), Malanjkhand (domain-I), J.N.Kote, Godhra, Chitradurga southern and northern granite, respectively. The eigen parameters are achieved by writing algorithms in MATLAB interface.

general increase in their vorticity number, i.e. the stronger the component of simple shear under which a particular region deforms, the greater is the angular shift of the V_2–V_3 plane from its MF plane's strike.

Seeking an explanation of this eccentricity observed in the above-mentioned two granitoids (Chakradharpur and Godhra), we analyse the modality of their data (K_3) distributions in Fig. 4. The histogram plots in Fig. 4 reveal that the declinations of K_3 appear to have been bimodal for Chakradharpur and Godhra (Fig. 4a, d), while an overall unimodality is prevalent for the other granitoids. In the next section, we elaborate on the role of the varying modality of data distributions to explain the connection between the orientations of V_2–V_3 and MF for the studied granitoids in light of their different deformation regimes.

Figure 5 depicts the Cartesian plot (in ***ln*** space) of S_2/S_3 vs S_1/S_2. The shape parameter (K) is equal to $\ln(S_1/S_2)/\ln(S_2/S_3)$. By analogy to the Flinn diagram, each plot in Figure 5 is divided into two regions by the line K = 1. The region K > 1 depicts the cluster shape of the distribution, while K < 1 denotes the girdle shape. It is envisaged that the K values of all the granitoids show the cluster shape of the distribution, except for the J. N. Kote granite. The K values for Chakradharpur and Chitrdurga are found to be comparable and lie close to a uniaxial clustering. The K value for the Godhra granite tends toward 1 and suggests a feeble clustering

of the K_3. Figure 6a presents a ternary diagram based on three indices, P (Point or Cluster), G (Girdle) and R (Random), that represent the three end members of fabric distribution patterns obtained from the normalized eigenvalues (S_1, S_2 and S_3). To measure their relative values, we use the following relationships (Vollmer, 1990):

$$P = (S_1 - S_2)$$

$$G = 2(S_2 - S_3)$$

$$R = 3S_3$$

The above indices range from 0 to 1 with P + G + R = 1. All the studied granitoids show a K_3 distribution pattern of less girdle (<50 %). The granitoid from Chitradurga North shows the most random K_3 distribution, while the Chakradharpur granitoid displays the least random distribution. The strength parameter (C) of K_3 is presented in Figure 6b. Any point in each solid line in this figure represents an equal strength value that increases away from the origin. A dataset having a perfectly uniform distribution will lie on the origin. Figure 6b shows that the J. N. Kote and Godhra bodies have the highest and lowest C values, respectively, thus indicating a maximum and minimum strength of their K_3 distribution.
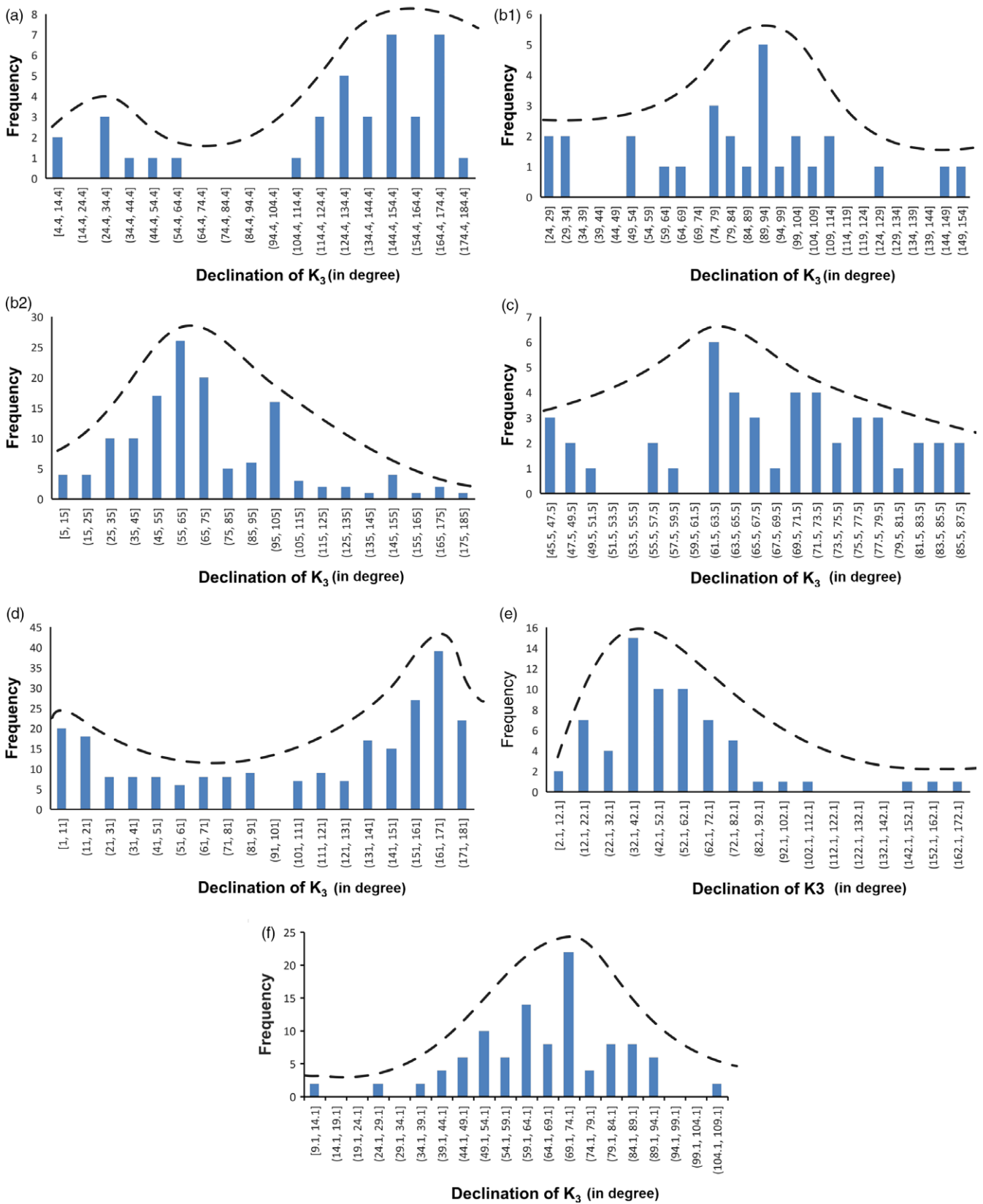
Fig. 4. (Colour online) (a), (b1), (b2), (c), (d), (e) and (f) are the histograms of declinations of magnetic foliation of Chakradharpur, Malanjkhand domain-II and -I, J. N. Kote, Godhra, Chitradurga southern and northern granite, respectively. (a) and (d) clearly show the bimodal distributions, while the rest remain overall unimodal.
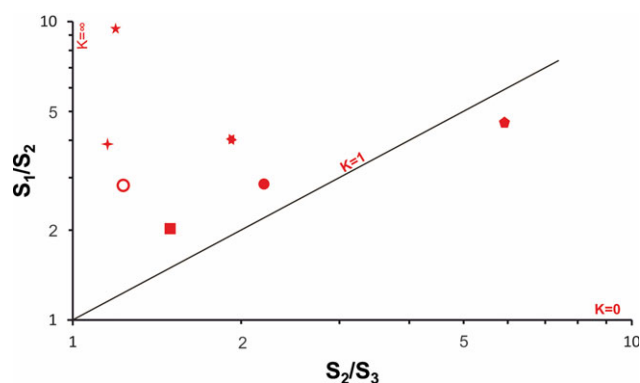
Fig. 5. (Colour online) The eigenvalue ratio graphs show the shape of magnetic foliation (K_3) data for all the granitoids. K denotes the shape parameter. The graph reads exactly same conventions of legends for different granites as is shown in Fig. 6.

The detailed discussion and conclusions from the above results are presented in Sections 6 and 7, respectively

6. Discussion

6.a. Estimating eigenvectors of magnetic fabric: a geometric approach coupled with mechanistic issues

Considering an individual magnetic foliation as a unit vector and following Scheidegger (1965), we primarily construct the 3×3 'orientation tensor matrix' (see also the discussion in Section 2) to compute three eigenvectors (V_1, V_2, V_3) and the normalized eigenvalues (S_1, S_2, S_3) associated with them. The above method has been applied for all the study areas, and therefore we obtain a different set of characteristic eigenvectors for each granitoid. Accordingly, assuming the individual datum of each distribution as a single point of unit mass within a sphere, an ellipsoid can be constructed. The three axes of the ellipsoid thus represent the direction of maximum, intermediate and minimum 'moment of inertia' of the assumed dissemination of masses. In such a scenario, Watson (1966) proposed that the direction of the maximum (V_1) and minimum (V_3) eigenvectors derived from an 'orientation tensor matrix' should follow the directions at which the 'moment of inertia' of the scattered masses is minimized and maximized, respectively.

For the magnetic fabric distributions in Malanjkhand (domain-II) and Chitradurga (south), the computed maximum eigenvectors (V_1) show consistency in tracing the direction of the mean pole to K_3, which leads to the coincidence between the strikes of V_2–V_3 and MF in these regions. Besides, the minimum eigenvectors (V_3) define the poles to their best-fit great circles (Fig. 3). Hence, the characteristics of the fabric eigenvectors obtained from these two granites conform very well to Watson's (1966) findings. However, in the rest of the cases, strikes of the V_2–V_3 planes show distinct angular variations with respect to the MF, thus not only contradicting our previous observations as well as Watson's (1966) propositions, but also instantly drawing additional attention to the mechanistic issues associated with the origin of their magnetic fabrics. Earlier AMS studies suggested that orientation of the mean magnetic foliation (MF) can be treated as an Instantaneous Stretching Axis (ISA_{max}) for syntectonic granitoids, that deformed under a steady-state material flow system (Mamtani *et al.* 2013; Mamtani, 2014; Mondal, 2018). Considering the analytical determination of the 2D vorticity of flow (Xypolias, 2010), these investigations also estimated vorticity numbers in the studied

granites, using (1) the angle between strikes of different planes (magnetic and field fabrics) on a horizontal plane, and (2) the parallelism between the direction of the shear zone and the extensional apophysis (A_e) of flow. It has been recorded that material flow in the Malanjkhand (domain-II), Chitradurga (south) and Godhra granitoid was close to the pure shear deformation, while simple shear was the dominant mechanism in the Malanjkhand (domain-I), J. N. Kote and Chitradurga (North) regions. Chakradharpur was the only granitoid that experienced general shear.

When correlating the above information with the obtained results, it can be physically accepted that the orientation of V_2–V_3, having been an estimation of the direction at which 'moment of inertia' of the distribution is maximized, should mimic the ISA_{max} of a particular steady-state flow under pure shear regime and retain its orientation throughout the all stages of progressive deformation. This is why the strikes of V_2–V_3 planes exactly coincide with that of MFs in Figure 3b1 and e. Contrasting this scenario, when the non-coaxial progressive deformations are considered, the rotational component of shear seems plausible to rotate the maximum eigenvector (V_1) from the direction of minimized 'moment of inertia'. Therefore, the rotational characteristics of eigenvectors with respect to a fixed coordinate on the stereonet physically explains the shift of V_2–V_3 orientation from MF (=ISAmax) in the simple-shear-dominated granitoids (e.g. Fig. 3b2, c and f). However, the results obtained from the Chakradharpur and Godhra granitoids (shaded region in Fig. 3) do not fit well with the above explanation as their V_2–V_3 planes also depict recognizable angular variations from ISA_{max} orientations in spite of their flows' being under general and pure shear regime, respectively. We would like to state that such discrepancies are attributed to the unique bimodal scattering (see Fig. 4a, d) pattern of their magnetic fabric distributions in comparison with rest of the granitoids. It may be noted that both the bimodality and the substantial amount of rotational strain contributed to shifting the V_2–V_3 from MF (or ISA_{max}) for Chakradharpur granitoid, while the former was considered to be the sole reason behind the noted strike mismatch of V_2–V_3 and MF in Godhra. We elaborate on these deficiencies of using the eigenvalue approach, which are related to the scattering pattern and symmetry classes of fabric data distribution, further in the next subsection (6.3).

It also seems important to mention here that the position of the V_2–V_3 plane may conveniently be used in the 2D vorticity analysis of any flow under pure shear deformation, as it stays the same along with the direction of ISA_{max} and does not rotate with respect to flow apophyses of extension (A_e = shear zone) throughout the entire history of progressive deformation. Nevertheless, the rotational tendency of the V_2–V_3 plane with respect to ISA_{max} as well as A_e during the progressive stages of deformation under any sub-simple/simple shear confirms their inadequacy when performing vorticity analysis from them. Therefore, we conclude that estimation of fabric eigenvectors as well as determination of their connection with respect to the direction of ISA_{max} (=MF plane), at least after checking the mode and symmetry of any fabric distribution over the stereonet, can be utilized as a powerful tool to determine the type of shear mechanism (i.e. pure or simple) associated with the steady-state material flow of any particular region.

6.b. Normalized eigenvalue ratios: an indicator of the strength of a deformation event

The strength parameter diagram (Fig. 6b) shows that none of the C values of the granitoids lie at the origin, which confirms that no
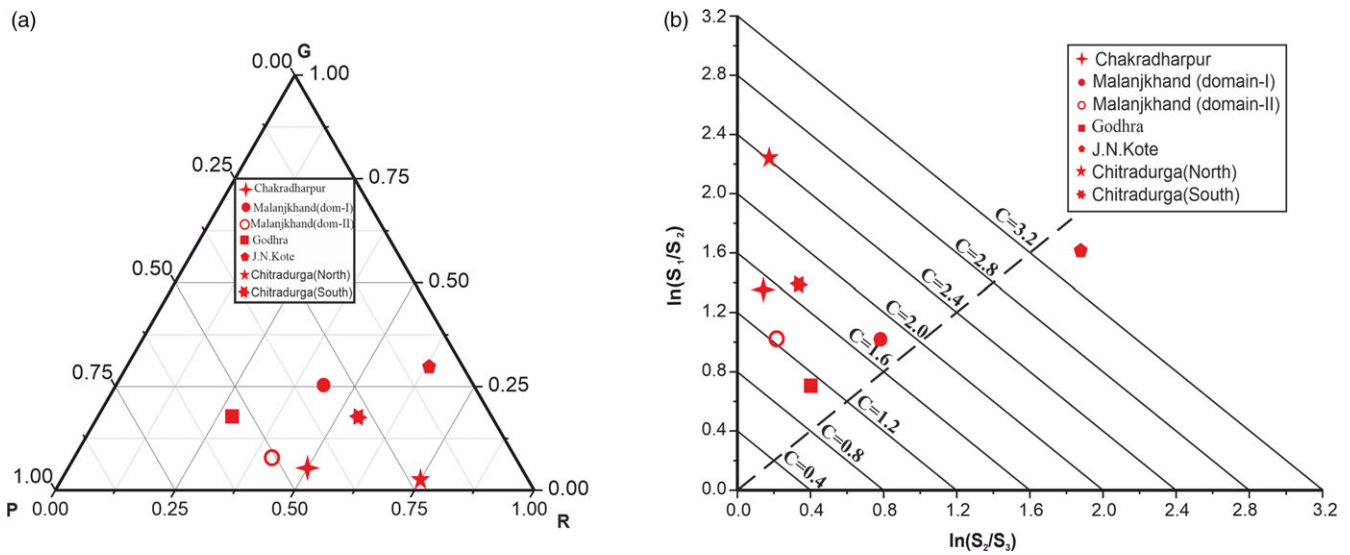
Fig. 6. (Colour online) (a) Ternary diagram, based on the indexes P (Point or Cluster), G (Girdle), R (Random) for all the granites. OriginLab (a data analysis and graphing software) was used to construct the ternary diagram. (b) The $\ln(S_1/S_2)$ vs $\ln(S_2/S_3)$ plot. C denotes the strength parameter. Note that Godhra and J. N. Kote granite show lowest and highest C values, respectively.

granitoid has magnetic foliation with a perfect uniform distribution. The arithmetical procedure used in the present paper to evaluate the strength parameters certainly shows its limitation when approaching with a structural dataset from poly-deformed regions. Since all the studied granitoids are known to have experienced more than one deformational event, we have consciously tried to incorporate the magnetic foliation data, as they manifest the late-stage deformation event only. It is evident from the figure that $C_{\text{J.N.Kote}} > C_{\text{Chitradurga(north)}} > C_{\text{Chitradurga(south)}} > C_{\text{Chakradharpur}} > C_{\text{Malanjkhand}} > C_{\text{Godhra}}$. This represents the sequence of the strength of K_3 data of all granitoid bodies.

Although there exists a prominent variation of sample numbers (n) in K_3 datasets for different granitoids, we assert that this would not anyway influence the reliability of obtained 'C' values in determining the strength parameters of magnetic fabrics. In accordance with Section 2 ('methodology' part), it may be noted that 'C' values are not computed directly from the eigenvalues (i.e. λ_i) but from their 'normalized' values (i.e. S_i), where $S_i = -\lambda_i/n$. Therefore, taking the summation over 'n' numbers of normalized direction cosines' product (i.e. components of the 'orientation tensor matrix') ultimately gives rise to $S_1 + S_2 + S_3 = 1$. In the current study, calculated values of S_i for all the granitoids truly satisfy this relation. This is why we infer that the variation of sample number (n) does not at all affect the calculated C values [$= (\ln(S_1/S_3)$] as well as our interpretation regarding the comparison of randomness for different granitoids.

6.c. Deficiencies of using eigenvalue approach in magnetic fabric analysis

The inconsistencies (associated with Fig. 3a, d) discussed in Subsection 6.1 clearly demand an overall realization of the limitations of using the eigenvalue method when analysing any structural fabric data that are relevant to coaxial or non-coaxial flows. In the present paper, all the analysis so far deals with the fabrics, which exhibit clusters with mainly orthorhombic symmetry. That the possibility of differences in modality may exist with individual clusters further leads us to plot the histograms of declinations of

K_3 in Fig. 4, separately for each granitoid. It may be noted that notwithstanding the rest of the granitoids, which more-or-less show unimodality, Chakradharpur and Godhra exhibit (Fig. 4a, d) a clear bimodal data distribution. This observation is found to be compatible with the observation made by Woodcock (1977) that for the bimodal or multimodal distributions, maximum eigenvector may not tend to exactly match the direction of the minimized 'moment of inertia'. We consider this to be one of the reasons behind the mismatch of strike orientation between the V_2–V_3 plane and ISA_{max} in these two granitoids (Fig. 3a, d). Apart from the modality of the data distributions, we would like to add that the other important factor which can induce such a mismatch is the symmetry of the fabric distributions. As stated before, all the granitoids exhibit overall orthorhombic symmetry, which is another essential condition (in addition to unimodality and coaxiality of deformation) behind the observed coincidence of V_2–V_3 with the direction of maximized 'moment of inertia' ($=\text{ISA}_{\text{max}}/\text{MF}$) in pure-shear-dominated regions (Fig. 3b1, e). Considering other fabric symmetries such as axial, spherical, monoclinic and triclinic (Turner & Weiss, 1963, pp. 43–4), the eigenvalue approach would be useful in identifying the ISA_{max} in only the first two cases as previous investigations confirmed the coaxiality between V_1 and the minimum 'moment of inertia' in such symmetries (Woodcock & Naylor, 1983). However, since the eigenvector analysis imposes an orthorhombic symmetry on the analysed data even if the distribution has a different kind of symmetry, extra attention should be paid when approaching with the monoclinic and triclinic data distribution. Therefore, although the examples of atypical granitoids, i.e. Chakradharpur and Godhra, serve the purpose of studying significant deficiencies of using the eigenvalue method in any structural fabric data analysis, we insist that, for any unimodal distribution of orthorhombic symmetry, estimation of fabric eigenvectors can be used to directly assess the style of deformation mechanism (pure/general/simple), whilst their corresponding eigenvalues provide some important aspects to decipher the fabric shape as well as strength of that deformation. In addition, considering the inadequacies of the eigenvalue

approach in the above-mentioned complexities, we must not deny the necessity of future research in this realm, which would quantify the shift of the maximum eigenvector from the minimized 'moment of inertia' and their relationship with the mechanistic issues involved in such cases.

7. Conclusions

In the current study, we have used the eigenvalue method to determine the shape and strength of the magnetic foliations in various granitoids from India. The study also highlights the relationship between the positions of the eigenvectors and the mode of shearing that are responsible for the development of the magnetic fabric.

Below we summarize the major findings of the present study:

1) The positional uniqueness of characteristic eigenvectors (V_1, V_2 and V_3) of magnetic fabrics can be concluded to be an important geometrical aspect, which directly indicates the mode of shearing (coaxial/general/non-coaxial)-related mechanistic issues associated with any particular deformed region. In the case of an orthorhombic unimodal fabric distribution of a syntectonic granitoid deformed under pure shear regime, the orientation of the V_2–V_3 plane exactly mimics that of the instantaneous stretching axis (ISA_{max}) of the steady-state material flow system associated with that deformation.

2) In contrast to the pure-shear-dominated granitoids, the V_2–V_3 plane shows its rotating tendency with respect to ISA_{max} and flow apophysis of extension (=shear zone) in the case of simple-shear-dominated granitoids.

3) The P, G and R ternary diagram is a representation which can simultaneously quantify and compare the randomness of the magnetic fabric distributions of different syntectonic granitoids.

4) K and C are two parameters which can be used to classify several datasets according to their shape and strength. These are also two representatives of the uniformity of any dataset.

References

Allmendinger RW, Cardozo NC and Fisher D (2013) *Structural Geology Algorithms: Vectors & Tensors.* Cambridge: Cambridge University Press, 289 pp.

Almqvist BS, Henry B, Jackson MJ, Werner T and Lagroix F (2014) Methods and applications of magnetic anisotropy: a special issue in recognition of the career of Graham J. Borradaile. *Tectonophysics* **629**, 1–5. doi: 10.1016/j.tecto.2014.06.002.

Benn K, Rochette P, Bouchez JL and Hattori K (1993) Magnetic susceptibility, magnetic mineralogy and magnetic fabric in a late Archaean granitoid-gneiss belt. *Precambrian Research* **63**, 59–81.

Bingham C (1974) An antipodally symmetric distribution on the sphere. *Annals of Statistics* **2**, 1201–25.

Borradaile G (2003) *Statistics of Earth Science Data: Their Distribution in Time, Space, and Orientation.* Berlin: Springer.

Borradaile GJ and Henry B (1997) Tectonic applications of magnetic susceptibility and its anisotropy. *Earth-Science Reviews* **42**, 49–93. doi: 10.1016/S0012-8252(96)00044-X.

Borradaile GJ and Jackson M (2004) Anisotropy of magnetic susceptibility (AMS): magnetic petrofabrics of deformed rocks. In *Magnetic Fabric: Methods and Applications* (ed. F Martín-Hernández), pp. 299–360. Geological Society of London, Special Publication no. 238. doi: 10.1144/GSL.SP.2004.238.01.18.

Bouchez JL (1997) Granite is never isotropic: an introduction to AMS studies of granitic rocks. In *Granite: From Segregation of Melt to Emplacement Fabrics* (eds JL Bouchez, DHW Hutton and WE Stephen), pp. 95–112. Dordrecht: Kluwer Academic Publishers.

Cardozo N and Allmendinger RW (2013) Spherical projections with OSXStereonet. *Computers & Geosciences* **51**, 193–205. doi: 10.1016/j.cageo.2012.07.021.

Cobbold PR and Gapais D (1979) Specification of fabric shapes using an eigenvalue method: discussion. *Geological Society of America Bulletin* **90**, 310–12. doi: 10.1130/0016-7606(1979)90<310:SOFSUA>2.0.CO;2.

Ferré EC, Gébelin A, Till JL, Sassier C and Burmeister KC (2014) Deformation and magnetic fabrics in ductile shear zones: a review. *Tectonophysics* **629**, 179–88. doi: 10.1016/j.tecto.2014.04.008.

Flinn D (1962) On folding during three-dimensional progressive deformation. *Quarterly Journal of the Geological Society, London* **118**, 385–433.

Flinn D (1965) On the symmetry principle and the deformation ellipsoid. *Geological Magazine* **102**, 36–45. doi: 10.1017/S0016756800053851.

Gomez-Rivas E, Bons PD, Griera A, Carreras J, Druguet E and Evans L (2007) Strain and vorticity analysis using small-scale faults and associated drag folds. *Journal of Structural Geology* **29**,1882–99. doi: 10.1016/j.jsg.2007.09.001.

Grasemann B, Fritz H and Vannay JC (1999) Quantitative kinematic flow analysis from the Main Central Thrust Zone (NW-Himalaya, India): implications for a decelerating strain path and the extrusion of orogenic wedges. *Journal of Structural Geology* **21**,837–53. doi: 10.1016/S0191-8141(99)00077-2.

Grégoire V, de Saint-Blanquat M, Nédélec A and Bouchez JL (1995) Shape anisotropy versus magnetic interactions of magnetite grains: experiments and application to AMS in granitic rocks. *Geophysical Research Letters* **22**, 2765–8.

Jelínek V (1981) Characterization of magnetic fabric of rocks. *Tectonophysics* **79**, T63–7. doi: 10.1016/0040-1951(81)90110-4.

Launeau P, Bouchez JL and Benn K (1990) Shape preferred orientation of object populations: automatic analysis of digitized images. *Tectonophysics* **180**,.201–11. doi: 10.1016/0040-1951(90)90308-U.

Launeau P and Robin PY (1996) Fabric analysis using the intercept method. *Tectonophysics* **267**, 91–119. doi: 10.1016/S0040-1951(96)00091-1.

Majumder S and Mamtani MA (2009) Magnetic fabric in the Malanjkhand Granite (central India): implications for regional tectonics and Proterozoic suturing of the Indian shield. *Physics of the Earth and Planetary Interiors* **172**, 310–23. doi: 10.1016/j.pepi.2008.10.007.

Mamtani MA (2014) Magnetic fabric as a vorticity gauge in syntectonically deformed granitic rocks. *Tectonophysics* **629**, 189–96. doi: 10.1016/j.tecto.2014.01.032.

Mamtani MA and Greiling RO (2005) Granite emplacement and its relation with regional deformation in the Aravalli Mountain Belt (India): inferences from magnetic fabric. *Journal of Structural Geology* **27**, 2008–29. doi: 10.1016/j.jsg.2005.06.004.

Mamtani MA, Pal T and Greiling RO (2013) Kinematic analysis using AMS data from a deformed granitoid. *Journal of Structural Geology* **50**, 119–32. doi: 10.1016/j.jsg.2012.03.002.

Mark DM (1973) Analysis of axial orientation data, including till fabrics. *Geological Society of America Bulletin* **84**, 1369–74. doi: 10.1130/00167606(1973)84<1369:AOAODI>2.0.CO;2.

Mark DM (1974) On the interpretation of till fabrics. *Geology* **2**,101–4. doi: 10.1130/0091-7613(1974)2%3C101:OTIOTF%3E2.0.CO;2.

Mark DM and Andrews JT (1975) A re-examination of the till fabrics and the origins of some 'cross-valley' moraines on Baffin Island. *Geologiska Föreningen i Stockholm Förhandlingar* **97**, 321–5. doi: 10.1080/11035897509454323.

Martín-Hernández F and Hirt AM (2003) The anisotropy of magnetic susceptibility in biotite, muscovite and chlorite single crystal. *Tectonophysics* **367**, 13–28.

Mondal TK (2018) Evolution of fabric in Chitradurga granite (south India): a study based on microstructure, anisotropy of magnetic susceptibility (AMS) and vorticity analysis. *Techtonophysics* **723**, 149–61. doi: 10.1016/j.tecto.2017.12.013.

Mondal TK, Bhowmick S, Das S and Patsa A (2020) Paleostress field reconstruction in the western Dharwar craton, south India: evidence from brittle faults and associated structures of younger granites. *Journal of Structural Geology* **135**, 104040. doi: 10.1016/j.jsg.2020.104040.

Mondal TK and Mamtani MA (2013) 3-D Mohr circle construction using vein orientation data from Gadag (southern India) – implications to recognize fluid pressure fluctuation. *Journal of Structural Geology* **56**, 45–56. doi: 10.1016/j.jsg.2013.08.005.

Mondal TK and Mamtani MA (2014) Fabric analysis in rocks of the Gadag region (southern India): implications for time relationship between regional deformation and gold mineralization. *Tectonophysics* **629**, 238–49. doi: 10.1016/j.tecto.2013.09.021.

Olivier P, Saint Blanquat M, Gleizes G and Leblanc D (1997) Homogeneity of granite fabrics at the metre and dekametre scales. In *Granite: From Segregation of Melt to Emplacement Fabrics* (eds JL Bouchez, DHW Hutton and WE Stephen)), pp. 113–27. Dordrecht: Kluwer Academic Publishers.

Owens WH (1973) Strain modification of angular density distributions. *Tectonophysics* **16**, 249–61. doi: 10.1016/0040-1951(73)90014-0.

Owens WH and Bamford D (1976) A discussion on natural strain and geological structure: magnetic, seismic, and other anisotropic properties of rock fabrics. *Philosophical Transactions of the Royal Society of London. Series A, Mathematical and Physical Sciences* **283**, 55–68. doi: 10.1098/rsta.1976.0069.

Parés JM, van der Pluijm BA and Dinarès-Turell J (1999) Evolution of magnetic fabrics during incipient deformation of mudrocks (Pyrenees, northern Spain). *Tectonophysics* **307**, 1–14.

Paterson MS and Weiss LE (1961) Symmetry concepts in the structural analysis of deformed rocks. *Geological Society of America Bulletin* **72**, 841–82. doi: 10.1130/0016-7606(1961)72[841:SCITSA]2.0.CO;2.

Pueyo EL, Román-Berdiel MT, Bouchez JL, Casas AM and Larrasoaña JC (2004) Statistical significance of magnetic fabric data in studies of paramagnetic granites. In *Magnetic Fabric: Methods and Applications* (ed. F Martín-Hernández), pp. 395–420. *Geological Society of London, Special Publication no. 238*.

Rochette P (1987) Magnetic susceptibility of the rock matrix related to magnetic fabric studies. *Journal of Structural Geology* **9**, 1015–20.

Sen K and Mamtani MA (2006) Magnetic fabric, shape preferred orientation and regional strain in granitic rocks. *Journal of Structural Geology* **28**, 1870–82. doi: 10.1016/j.jsg.2006.07.005.

Simpson C and De Paor DG (1993) Strain and kinematic analysis in general shear zones. *Journal of Structural Geology* **15**, 1–20. doi: 10.1016/0191-8141(93)90075-L.

Scheidegger AM (1965) On the statistics of the orientation of bedding planes, grain axes, and similar sedimentological data. *US Geological Survey Professional Paper* **525C**, 164–7.

Tarling D and Hrouda F eds. (1993) *Magnetic Anisotropy of Rocks*. Dordrecht: Springer Science & Business Media.

Terrinha P, Pueyo EL, Aranguren A, Kullberg JC, Kullberg MC, Casas-Sainz A and Azevedo MDR (2017) Gravimetric and magnetic fabric study of the Sintra Igneous complex: laccolith-plug emplacement in the Western Iberian passive margin. *International Journal of Earth Sciences* **107**, 1807–33.

Tikoff B and Fossen H (1995) The limitations of three-dimensional kinematic vorticity analysis. *Journal of Structural Geology* **17**, 1771–84. doi: 10.1016/0191-8141(95)00069-P.

Trindade RI, Raposo MIB, Ernesto M and Siqueira R (1999) Magnetic susceptibility and partial anhysteretic remanence anisotropies in the magnetite-bearing granite pluton of Tourão, NE Brazil. *Tectonophysics* **314**, 443–68.

Turner FJ and Weiss LE (1963) *Structural Analysis of Metamorphic Tectonites*. New York: McGraw-Hill.

Vollmer FW (1990) An application of eigenvalue methods to structural domain analysis. *Geological Society of America Bulletin* **102**, 786–91. doi: 10.1130/0016-7606(1990)102<0786:AAOEMT>2.3.CO;2.

Wallis S (1995) Vorticity analysis and recognition of ductile extension in the Sanbagawa belt, SW Japan. *Journal of Structural Geology* **17**, 1077–93. doi: 10.1016/0191-8141(95)00005-X.

Watson GS (1966) The statistics of orientation data. *Journal of Geology* **74**, 786–97. doi: 10.1086/627211.

Williams GD and Chapman TJ (1979) The geometrical classification of non-cylindrical folds. *Journal of Structural Geology* **1**, 181–5. doi: 10.1016/0191-8141(79)90038-5.

Woodcock NH (1977) Specification of fabric shapes using an eigenvalue method. *Geological Society of America Bulletin* **88**, 1231–6. doi: 10.1130/0016-7606(1977)88<1231:SOFSUA>2.0.CO;2.

Woodcock NH and Naylor M (1983) Randomness testing in three-dimensional orientation data. *Journal of Structural Geology* **5**, 539–48. doi: 10.1016/0191-8141(83)90058-5.

Xypolias P (2010) Vorticity analysis in shear zones: a review of methods and applications. *Journal of Structural Geology* **32**, 2072–92. doi: 10.1016/j.jsg.2010.08.009.